

Synchronised Bus-Clamping PWM Strategies based on Space Vector Approach for Modulation upto Six-Step Mode

G.Narayanan V.T.Ranganathan

Department of Electrical Engg., Indian Institute of Science, Bangalore, INDIA
email : gnar@ee.iisc.ernet.in vtran@ee.iisc.ernet.in

Abstract

Synchronised PWM waveforms with 3-phase, half-wave and quarter-wave symmetries are required in VSI-fed, high-power ac drives. The flexibilities of the space vector approach to modulation can be utilised for real-time generation of more than one family of synchronised PWM waveforms, maintaining all the symmetries, with any odd pulse number. Two such synchronised PWM strategies are proposed in this paper along with an overmodulation scheme for operation upto six-step mode, maintaining the modulator gain constant in the whole range. The proposed overmodulation scheme does not require any evaluation of quadratic or cubic expressions, or any look-up table except for storing sine values. These two strategies result in a harmonic distortion better than those of comparable ones at higher modulation indices for low pulse numbers of 5 and 7. A combination of these two strategies, along with two other bus-clamping strategies and the conventional space vector strategy, leads to a significant reduction in the harmonic currents in constant V/f induction motor drives as shown by the theoretical as well as experimental results.

Key words : Synchronised PWM, space vector, induction motor, high-power drives.

1. Introduction

Pulsewidth Modulation (PWM) strategies, employed in high-power ac drives, must generate synchronised PWM waveforms with 3-Phase Symmetry (3PS), Half Wave Symmetry (HWS) and Quarter Wave Symmetry (QWS) so as to keep the harmonics and their undesirable effects to a minimum. The ratio of the switching frequency (f_{sw}) of the inverter to the fundamental modulating frequency (f_1), or the pulse number ($p_{sw} = f_{sw}/f_1$), must be an odd multiple of 3 to maintain the symmetries in synchronised sine-triangle PWM and synchronised conventional space vector PWM [1]. However, using the idea of "bus-clamping" [1-4] and exploiting the flexibilities of the space vector approach to

modulation [3,4], it is possible to generate more than one family of synchronised PWM waveforms, maintaining all the symmetries, with any odd pulse number as will be demonstrated in the later sections.

The principles involved in such space vector-based, real-time synchronised PWM and a few PWM strategies based on these principles were presented recently [3,4]. Besides presenting the relevant details about these, two more such synchronised bus-clamping PWM strategies are proposed in this paper. An overmodulation scheme for operation upto six-step mode is also proposed for these two strategies. Also, the modulator gain is maintained constant upto the six-step mode. These strategies are well-suited for digital implementation.

Space vector-based overmodulation schemes [5-7] and schemes for linearising the modulator gain in the overmodulation range [8] involve non-linear expressions to be computed. These are usually stored as look-up tables or approximated to quadratic or cubic expressions. However, in the present work, these expressions are not very non-linear that have been linearised with a reasonable accuracy. Hence, no look-up table other than the sine table and no computation of quadratic or cubic expressions are involved.

These bus-clamping PWM strategies result in a better harmonic distortion than the conventional space vector strategy at higher modulation indices. These strategies can be utilised in combination with the conventional space vector strategy at appropriate speed ranges to reduce the harmonic currents, torque pulsation etc. in constant V/f induction motor drives, subject to different values of maximum switching frequencies ($f_{sw(max)}$) of the inverter.

2. Space vector approach to synchronised PWM

Let modulation index (M) be defined as $M = V_1 / V_{1(6\text{-step})}$, where V_1 is the fundamental

voltage generated and $V_{1(6\text{-step})}$ is the fundamental voltage obtained during 6-step operation with the same dc bus voltage.

Given a reference vector of normalised magnitude 'a' at steady-state, the relationship a vs. M is non-linear in the range $a > 0.866$. Even in the range $a \leq 0.866$, with low sampling frequencies, this relationship may not be linear. This work aims at real-time generation of synchronised PWM waveforms with all the symmetries with

1. the reference vector sampled at a uniform rate and
2. the proportionality $a = (0.866/0.907) * M$ maintained in the whole range of M, i.e. $M \leq 1$ or $a \leq 0.955$, and even with low sampling rates.

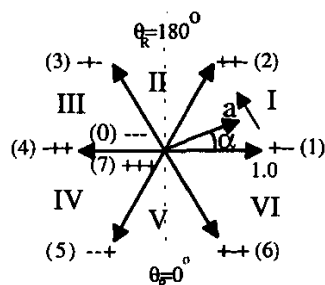


Fig. 1a Voltage space vectors produced by an inverter
 $\theta_R =$ Angle of R-phase fundamental voltage

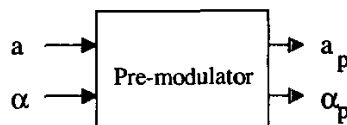


Fig. 1b Pre-modulation

The reference vector is sampled once in every subcycle T_s , "pre-modulated" as shown in Fig. 1 and the durations of different states are calculated. The calculations are done in sector I as shown in Eqn. (1). The pre-modulation is done such that the proportionality is maintained between 'a' and M.

$$\begin{aligned} T_1 &= a_p * T_s * \sin(60^\circ - \alpha_p) / \sin(60^\circ) \\ T_2 &= a_p * T_s * \sin(\alpha_p) / \sin(60^\circ) \\ T_0 + T_7 &= T_s - T_1 - T_2 \end{aligned} \quad (1)$$

The pre-modulated samples must be at identical positions in every sector. Switching sequences (e.g 0-1-2-7, 0-1-2, 1-2-7 etc.) corresponding to every pre-modulated sample

must be identified satisfying the conditions for the symmetries brought out in Table 1 as well as the following two rules:

- (a) Only one switching per state transition.
- (b) Not more than 3 switchings per sample.

$s(90^\circ - \theta)$, $0^\circ < \theta < 60^\circ$	$s(270^\circ - \theta)$ for HWS	$s(210^\circ - \theta)$ for 3PS	$s(150^\circ - \theta)$ for HWS & 3PS	$s(90^\circ + \theta)$ for QWS & 3PS
--	+++	--	+++	--
+++	--	+++	--	+++
+--	--	--	++	+--
++	++	++	+--	++

Table 1a. Combining the conditions for QWS, HWS and 3PS

$s(120^\circ - \phi)$, $0^\circ < \phi < 30^\circ$	$s(120^\circ + \phi)$ $0^\circ < \phi < 30^\circ$
--	+++
+++	--
+--	++
++	+--

Table 1b. Conditions for the symmetries as applicable in sector I

In conventional space vector PWM strategy (CSVPWM), Basic Bus-Clamping Strategy-I (BBCS-I) and Boundary Sampling Strategy-I (BSS-I) [3,4], there must be a sample at $\alpha_p = 30^\circ$, generated using the sequence 0-1-2-7 or 7-2-1-0 in sector I. The positions of the other samples are symmetrical about this sample. The sequences used for these satisfy the above conditions, and result in bus-clamping in case of BBCS-I and BSS-I. BSS-I uses a 'boundary sample' at $\alpha_p = 0^\circ$, generated using the sequence 0-1-0 or 1-0-1. The desired positions of the samples are ensured in the sampling stage itself or in the pre-modulation stage.

In CSVPWM, n_s must be odd, and $p_{sw} = 3n_s = 3, 9, 15, 21, \dots$ for the waveforms generated. In BBCS-I, n_s must be odd, and $p_{sw} = 2n_s + 1 = 3, 7, 11, 15, \dots$. In BSS-I, n_s must be even, and $p_{sw} = 2n_s + 1 = 5, 9, 13, 17, \dots$

3. Proposed strategies

The two proposed strategies also have samples positioned symmetrically about the centre of the sector. But, unlike the earlier strategies, the proposed strategies do not have a sample at $\alpha_p = 30^\circ$. Instead they have two samples at the middle of the sector, one at α_{m1} and the other at α_{m2} such that $(30^\circ - \alpha_{m1}) = (\alpha_{m2} - 30^\circ)$, which use the

pair of sequences (0-1-2, 1-2-7) or (7-2-1, 2-1-0) in sector I, and thereby change the zero state used once in every sector at the middle of the sector.

3.1 Basic Bus Clamping Strategy-II(BBCS-II)

This strategy has $(n_s-2)/2$ samples located symmetrically on either side of the two samples at the centre. This results in an even-valued n_s . Hence $p_{sw}=2n_s+1=5,9,13,17\dots$ for the waveforms generated.

3.2 Boundary Sampling Strategy-II (BSS-II)

Combining the ideas of the earlier BBCS-II and boundary sampling, this strategy can be arrived at. This strategy has an even number of samples within the sector boundaries and a sample on every sector boundary. Here, $n_s=3,5,7,9\dots$, and $p_{sw}=7,11,15,19\dots$

3.3 Zones of modulation

An average voltage vector (V_{av}) is generated in every subcycle. The different zones of modulation can be identified in terms of the magnitudes and positions of V_{av} generated during different subcycles over a cycle or a sector.

In the lower ranges of M , the magnitude of V_{av} remains the same in every subcycle over a cycle at steady-state, while only the angle changes in equal steps. The tip of the average vectors during the different subcycles lie on a circle. Hence this zone can be called 'circular modulation zone'. M is increased by increasing the magnitude of V_{av} till the latter equals 0.866, beyond which is the 'overmodulation zone'. A popular approach to overmodulation is the 2-zone approach [5]. An alternative approach has been recently proposed [6,7], but the performance of this is inferior [6].

In any subcycle, the tip of the average vector generated can lie only within or on the hexagon connecting the tips of the voltage vectors produced by the inverter. In overmodulation zone-I, closer to the sector boundaries, the tips of V_{av} generated during the different subcycles, lie within the hexagon and on a circle. On the other hand, around the middle of the sectors, they lie on the hexagon. In overmodulation zone-II, in every subcycle the tip of the average vector lies on the hexagon.

3.4 Premodulation

It is ensured that the positions of the samples are as required to meet the conditions for symmetry as discussed in the earlier sections. The sample is then pre-modulated. The pre-modulated sample corresponds to the average vector generated in the given subcycle. The pre-modulation process depends on the zone of modulation, which is identified from 'a'. In the different zones, it is done as follows.

3.4.1 Circular modulation zone

The premodulation does not change the position of the sample in this zone. Only in case of low pulse numbers of 5 and 7, pre-modulation is required. The non-linear relationship a vs. a_p is linearised, and if needed, piecewise. Using this linearised relationship, 'a' is corrected as follows:

$$\alpha_p = \alpha$$

$$a_p = k_{mag1} * a + c_{mag1} \quad (2)$$

3.4.2 Overmodulation zone-I

M is increased by increasing the radius of the circular portion of the trajectory of the tip of pre-modulated vector (a_{cir}) in zone-I. a_{cir} vs. a is linearised and used to compute a_{cir} . Using α_p and a_{cir} , a_p is then determined as follows :

$$\alpha_p = \alpha$$

$$a_{cir} = k_{mag2} * a + c_{mag2}$$

$$a_p = a_{cir}, \text{ if the tip of pre-modulated sample lies on the circle}$$

$$a_p = 0.866/\cos(30^\circ - \alpha_p), \text{ if the tip lies on the hexagon.} \quad (3)$$

3.4.3 Overmodulation zone-II

M is increased in this zone, by shifting the pre-modulated samples closer to the nearest sector boundary. The relationship between k_{ang} and 'a' is linearised. This linearised expression is used to compute k_{ang} , the angle correction factor. α is corrected using k_{ang} . a_p is then computed using α_p .

$$k_{ang} = k_a * a + c_a$$

$$\alpha_p = k_{ang} * \alpha, \text{ if } 0^\circ < \alpha < 30^\circ$$

$$\alpha_p = 60^\circ - k_{ang} * (60^\circ - \alpha), \text{ if } 30^\circ < \alpha < 60^\circ$$

$$a_p = 0.866/\cos(30^\circ - \alpha_p) \quad (4)$$

The error in M due to any of the above linearisations is less than 0.005.

4. Equivalent carrier and modulating waves

The variations of the average pole-voltage over the fundamental cycle for BSS-II, $n_s=3$, $p_{sw}=7$ at

M=0.9 and 0.7 respectively are shown in solid lines and dashed and dotted lines in Fig.2a. Similar waveforms are shown for BSS-II, $n_s=5$, $p_{sw}=11$ in Fig. 2b.

The modulating waves used in classical triangle-comparison methods are nothing but the variation of average pole-voltage over the fundamental cycle. Hence, the above waveforms can be taken as modulating waves, and can be compared with suitable carrier waves to generate the same PWM waveforms. Now, these carrier waves are not the regular, isocles triangular carrier waves, but ones which are irregular and discontinuous as shown in dashed lines in Figs. 3a and 3b. Also, given a modulation index M, the triplen frequency components to be added to the fundamental to get the modulating wave are not very obvious, especially due to boundary sampling.

However, this modulation process is easily conceived and implemented using the space vector approach due to the flexibilities like multiple switching of a phase within T_s , the choice of dividing a sector into either an odd or even number of subcycles without losing the symmetries etc. Thus, these strategies are very different from the ones proposed in the literature, which just utilise the degree of freedom in the division of the total duration of zero vector between the states 0 and 7 [1,2].

5. Results

The performance of the proposed strategies are evaluated in this section. The usefulness of these strategies in improving the performance of constant V/f induction motor drives is demonstrated both theoretically as well as experimentally.

5.1 Performance evaluation

The total harmonic distortion factor of the no-load current waveform (I_{THD}) is a suitable performance index for high-power, VSI-fed ac drives [9]. An equivalent quantity, independent of the machine parameters and load conditions, is the weighted total harmonic distortion factor of the line-line voltage waveform (V_{WTHD}).

$$I_{THD} = \frac{1}{I_1} \sqrt{\sum (I_n)^2}, V_{WTHD} = \frac{1}{V_1} \sqrt{\sum \left(\frac{V_n}{n}\right)^2}, n \neq 1$$

5.1.1 V_{WTHD} vs. M characteristics

BBCS-II leads to lesser V_{WTHD} at higher M compared to BSS-I for $p_{sw}=5$, while BSS-II leads to lesser V_{WTHD} at higher M compared to BBCS-I for $p_{sw}=7$ as shown in Fig.3a. Also, the V_{WTHD} is less than that due to 6-step operation, i.e. 0.046, only with the two proposed strategies over a considerable range of M. Thus, the two proposed strategies perform better at higher M.

5.2.2 Torque pulsation

As the PWM waveforms generated are synchronised ones, their spectra are discrete. As HWS is maintained, there are no even harmonics. Hence, harmonic currents of order 5,7,11,13,17,19... only flow through the motor windings. As 3PS is maintained, every frequency component is balanced, resulting in torque pulsations of order 6,12,18... only. The sixth harmonic torque (T_6), for instance, is approximately proportional to $I_5 \sim I_7$ [10]. Hence, $(V_5/5) \sim (V_7/7)$ gives a measure of T_6 . Similarly, for other harmonic torques.

Like V_{WTHD} , $(V_5/5) \sim (V_7/7)$ is a quantity independent of the motor parameters and the load conditions, and can be used to compare the performances of two strategies in terms of the sixth harmonic torque at any given M. Similarly, for other harmonic torques.

$(V_5/5) \sim (V_7/7)$ is computed and plotted for the two proposed strategies and the two comparable strategies as a function of M as shown in Fig. 3b. It can be seen that the proposed strategies perform better at higher M.

5.2 Application to V/f drives

Different PWM strategies generate PWM waveforms with different pulse numbers, and perform better in different ranges of M. Hence, subject to any maximum switching frequency limit ($f_{sw(max)}$) on the inverter, a hybrid PWM can be proposed, which employs different strategies with different pulse numbers over different ranges of speed in a constant V/f drive. The hybrid PWM can aim at either a reduction in harmonic distortion or torque pulsation in different speed ranges of the drive. In the present work, a reduction in harmonic distortion is aimed at.

For a constant V/f drive with $f_{sw(max)}=250\text{Hz}$ and a base frequency of 50Hz, the proposed hybrid PWM results in a significant reduction in

Fig.2 Equivalent carrier and modulating waves

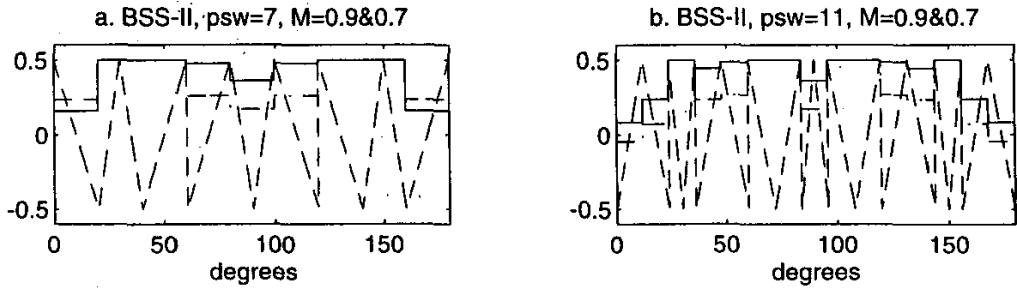


Fig.3a Vwthd vs.M

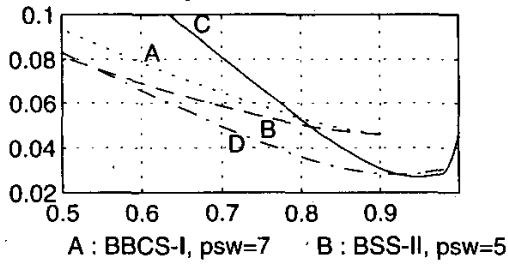


Fig.3b Sixth harmonic torque vs.M

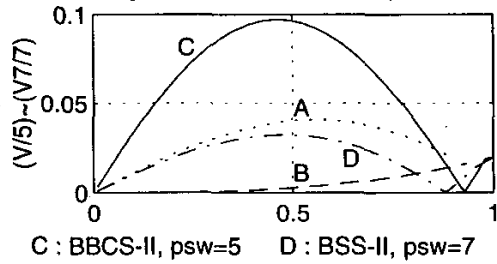


Fig.4a Vwthd vs.f1 of drive

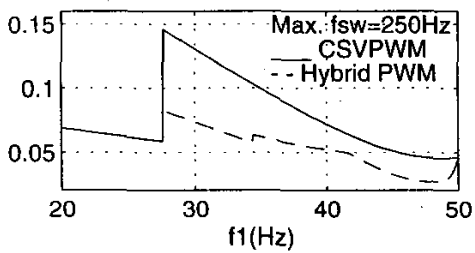


Fig.4b Measured lthd vs.f1 of drive

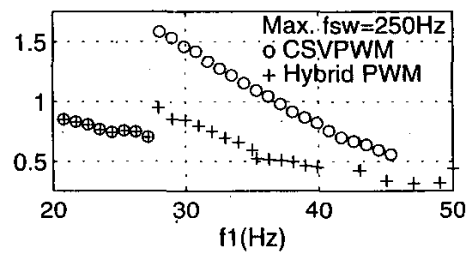
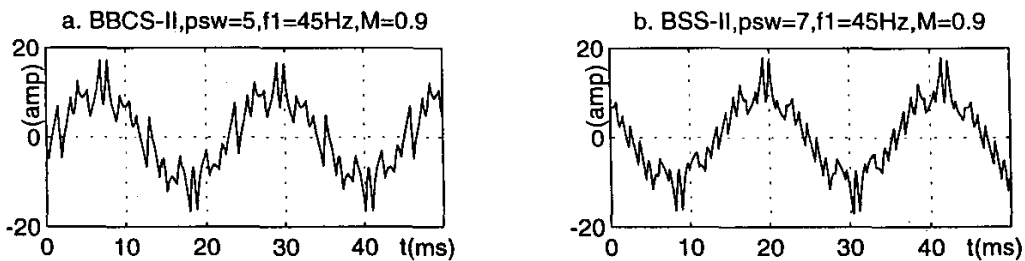


Fig.5 Experimental no-load current waveforms



V_{WTHD} in the speed range of 27.8Hz to 50Hz as compared to CSVPWM as shown in Fig.4a . The percentage reduction in V_{WTHD} tallies with the reduction in I_{THD} measured experimentally on a 3kW, 200V, 50Hz, 3-phase induction motor drive, fed from an IGBT-based, 5kVA inverter. The measured I_{THD} values are as shown in Fig. 4b. Some experimental no-load current waveforms are shown in Fig.5 .

To maintain V_{WTHD} to be less than that of six-step mode, namely 0.046, in the whole speed range, off-line optimised PWM [1] requires the f_{sw} rating of the inverter to be around 320Hz. Among the real-time strategies, the f_{sw} rating required in case of synchronised sine-triangle PWM and synchronised conventional space vector PWM are as high as 650Hz and 525Hz respectively. On the other hand, with the proposed techniques, the f_{sw} rating required is only around 375Hz, which is much superior to those of the two conventional strategies and fairly close to that of the off-line optimised PWM.

6. Conclusion

Two space vector-based, synchronised, bus-clamping PWM strategies, namely BBCS-II and BSS-II, are proposed along with an overmodulation scheme for operation upto six-step mode. The two proposed strategies perform better than other such strategies at higher M with $p_{sw}=5$ and 7. A combination of these two strategies, together with BBCS-I, BSS-I and CSVPWM, can significantly reduce the harmonic distortion or torque pulsation in constant V/f drives. The reduction achieved in the harmonic distortion is shown theoretically as well as experimentally.

References

1. J.Holtz, "Pulsewidth modulation for electronic power conversion", Proc. IEEE, 1994, **82**(8), pp.1194-1214.
2. V.Blasko, "Analysis of a hybrid PWM based on modified space-vector and triangle-comparison method", IEEE Trans., 1997, **IA-33**(3), pp. 756-764.
3. G.Narayanan and V.T.Ranganathan, "Synchronised PWM generation based on space vector approach. Part I : Principles of waveform

generation", accepted for publication in IEE Proc.B.

4. __, "Synchronised PWM generation based on space vector approach. Part II : Application to V/f drives", accepted for publication in IEE Proc.B.
5. J.Holtz, W.Lotzkat and A.Khambadkone, "On continuous control of PWM inverters in the overmodulation range including six-step mode", Proc. IECON, 1992, pp.307-312.
6. S.Bolognani and M.Zigliotto, "Space vector Fourier analysis of SVM inverters in the overmodulation range", Proc. PEDES, 1996, pp. 319-323.
7. __, "Novel digital continuous control of SVM inverters in the overmodulation range", IEEE Trans., 1997, **IA-33**(2), pp. 525-530.
8. V.Kaura, "A new method to linearise any triangle-comparison-based PWM by reshaping the modulation command", IEEE Trans., 1997, **IA-33**(5), pp. 1254-1259.
9. H.Stemmler, "High-Power Industrial Drives", Proc. IEEE, 1994, **82**(8), pp. 1266-1286.
10. S.D.T.Robertson and K.M.Hebbar, "Torque pulsations in induction motors with inverter drives", IEEE Trans., 1971, **IGA-7**(2), pp. 318-323.